

PNA-TPP Targeting Drp1 of Lung Adenocarcinoma Cancer Stem Cells Enhance the Sensitivity to Cisplatin

Lixia Xie

The Second Affiliated Hospital of Nanchang University

Yong Cheng

The Second Affiliated Hospital of nanchang University

Ping Hu

The Second Affiliated Hospital of Nanchang University

Xiaoqun Ye (✉ 511201663@qq.com)

The Second Affiliated Hospital of Nanchang University

Research Article

Keywords: PNA TPP, Drp1, CSCs, Targeted therapy

Posted Date: May 6th, 2021

DOI: <https://doi.org/10.21203/rs.3.rs-452487/v1>

License:  This work is licensed under a Creative Commons Attribution 4.0 International License.

[Read Full License](#)

1
2
3
4
5
6
7
8
9
10
11
12
13
14
15
16
17
18
19
20
21
22
23
24
25
26
27
28
29
30
31
32
33
34
35
36
37
38
39
40
41
42
43
44

PNA-TPP targeting Drp1 of lung adenocarcinoma cancer stem cells enhance the sensitivity to cisplatin

Lixia Xie¹, Yong Cheng¹, Ping Hu¹, Xiaoqun Ye^{1*}

¹Department of Respiratory Diseases, The Second Affiliated Hospital of Nanchang University, Nanchang, China

* Xiaoqun Ye, 511201663@qq.com. Department of Respiratory Diseases, The Second Affiliated Hospital of Nanchang University, Nanchang, China

45 **Abstract**

46 The presence of cancer stem cells (CSCs) is the source of occurrence, aggravation, and recurrence of
47 lung cancer. Accordingly, targeting the lung CSCs has been suggested to be an effective approach for
48 lung cancer treatment. Mitochondrial dynamics are currently considered to be closely related to
49 apoptosis. Drp1 is the key component of the mitochondrial fission machinery. Our study indicated that
50 peptide nucleic acid (PNA) promoting dynamic-related protein 1 (Drp1) expression improved cell
51 apoptosis and the sensitivity to cisplatin (CDDP) in lung adenocarcinoma cancer stem cell.
52 Interestingly, overexpression of Drp1 had a similar effect with PNA, and knockdown of Drp1 did the
53 opposite. These data suggested that PNA promote cell apoptosis and enhance the sensitivity to CDDP
54 of lung CSCs via Drp1. It will be of great interest to further explore the therapeutic strategies of lung
55 cancer.

56

57 **Keywords**

58 PNA-TPP, Drp1, CSCs, Targeted therapy

59

60 **Introduction**

61 Lung cancer is the malignant tumor with the highest morbidity and mortality rate in the world. Only 18%
62 of all patients with lung cancer are alive 5 years or more after diagnosis¹. Adenocarcinoma is the most
63 common histologic subtype of NSCLC for which chemotherapy is an common but important method of
64 the treatment¹. However, the drug resistance as developed during the course of therapy really limits the
65 efficacy of chemotherapy. According to some studies, there exists a fraction of stem-like cells in tumor
66 namely cancer stem cells (CSCs) which are the root of tumor growth, relapse, metastasis and drug
67 resistance. In general, although conventional chemotherapeutic agents eliminate the majority of tumor
68 cells, CSCs spared are capable of forming the heterogenic tumor mass^{2,3}. Therefore, it is urgent to
69 explore a effective treatment for targeting lung cancer stem cells.

70 Studies have shown that, mitochondrial fission has also been associated with a broad range of cell
71 processes, such as apoptosis, mitochondrial biogenesis, mitophagy, cell proliferation, differentiation
72 and transformation⁴. Ye et al. found that there was no significant change in the number of mitochondria
73 in A549 stem cell spheres, in which mitochondrial fission decreased and fusion increased⁵.
74 Mitochondrial fission is currently considered to be closely related to apoptosis and chemotherapy
75 sensitivity in cancer cells⁶⁻⁸. Studies had shown that cisplatin resistance in cholangiocarcinoma was
76 associated with mitochondrial dynamics, and mitochondrial fission induced apoptosis⁹. Mitochondrial
77 fission is usually associated with decreased mitochondrial membrane potential, but it is usually
78 recoverable. However, if the stress is too strong, the mitochondrial membrane potential cannot be
79 restored and can be degraded by mitochondrial autophagy or eventually lead to apoptosis.

80 PNA, a DNA molecule analogue, in which sugar-phosphate backbone is instead by a pseudopeptide
81 backbone composed of N-(2-aminoethyl)glycine units, can resistant to hydrolytic and enzymatic
82 cleavage¹⁰. PNAs can specifically recognize complementary DNA obeying Watson-Crick base-pairing
83 rules to form a stable helix¹¹. Studies shown that specific peptide nucleic acid fragments targeting
84 tumor-associated oncogene mutation genes, mitochondrial mutation genes, and epidermal growth
85 factor receptor genes (EGFR) can inhibit growth of tumors such as melanoma, head, neck squamous
86 cell carcinoma (HNSCC), non-small cell lung cancer (NSCLC), NCI-H446, breast cancer cell and
87 human choriocarcinoma JAR Cells¹²⁻¹⁵. Mitochondrial DNA is a closed loop double-stranded DNA
88 molecule, including the outer loop (heavy-strand promoter, HSP) and the inner loop (light-strand

89 promoter, LSP), which encodes oxidative phosphorylation related proteins including 12 species (ATP6
90 and ATP8, etc.) and 1 species (ND6), respectively¹⁶. Notably, both LSP and HSP are localized in
91 D-loop regulatory region, making it a presumptive target for PNA interference. We thus designed a
92 PNA for D-loop targeting, coupled with triphenylphosphonium (TPP), a delocalized lipophilic cation
93 for mitochondria targeting^{17,18}. Our groups had demonstrated that the given PNA-TPP significantly
94 disrupted mitochondrial gene expression, resulting in cell death and enhancing chemosensitivity of
95 cisplatin¹⁹. However, the specific mechanism of PNA-TPP promoting apoptosis of lung cancer stem
96 cells and enhancing chemosensitivity of cisplatin is unknown.

97 In our study, firstly, resorting to the high mitochondrial membrane potential of the lung cancer cell line
98 A549, we used PNA-TPP to block its mitochondrial DNA double-strand promoter consensus gene and
99 disrupt the mitochondrial energy metabolism. Then we researched its influence on cAMP/PKA/Drp1
100 pathway, mitochondrial fission, ROS generation, chemosensitivity of cisplatin. The lentiviral
101 transfection technique was used to alter the expression of Drp1 protein in the mitochondria of A549
102 cell spheres, and to investigate whether it affected the level of intracellular ROS and apoptosis. The
103 research results are expected to provide new ideas and experimental basis for targeting the removal of
104 lung adenocarcinoma stem cells and improving the clinical comprehensive therapeutic effect of lung
105 adenocarcinoma.

106 **Materials and methods**

107

108 **Reagents and antibodies**

109 Cell culture products including Dulbecco's modified Eagle's medium (DMEM)/High
110 Glucose, DMEM/F-12 and fetal bovine serum (FBS) were obtained from Biological Industries (Israel).
111 Trypsin and EDTA were obtained from Solarbio (Beijing, China), B27 was purchased from Gibco
112 (Grand Island, NY, USA), EGF and bFGF were obtained from Peprotech (Rocky Hill, USA). PKA-C α
113 and Drp1 Rabbit mAb antibody was obtained from Cell Signaling Technology (Danvers, MA); Bcl-2
114 and BAX Rabbit mAb antibody and β -actin mouse mAb antibody were purchased from proteintech
115 (Wuhan, China). The cell counting kit-8 (CCK-8), goat anti-mouse/rabbit IgG (H&L) were purchased
116 from Transgen Biotech (Beijing, China); the Annexin V-APC/PI apoptosis detection kit was obtained
117 from keygen biotech (Nanjing, China); Western blot reagents were obtained from Bio-Rad Laboratories
118 (Hercules, CA), and the Pierce BCA Protein Assay Kit was purchased from Applygen Technologies Inc
119 (Beijing, China).

120

121 **Cell line**

122 The human NSCLC cell line A549 was obtained from the Second Affiliated Hospital of Nanchang
123 university stored in liquid nitrogen preservation equipment and cultured in high glucose/DMEM
124 supplemented with 10%FBS (v/v), streptomycin and penicillin , incubated with 5% CO₂ at 37°C. A549
125 cell spheres were cultured using technique method as previously described. In a nutshell, A549 cells
126 were seeded in the 6-well plates with 1000-1500 cells per well in 2ml 10%FBS/DMEM for 8-10 days.
127 Thereafter, clones, namely meroclones, paraclones and holoclone, may formed, in which the latter
128 possessing of some stem cell characteristics like continuous passage, and unlimited proliferation. So we
129 next collected the holoclone cells and exchanged to culture in serum-free stem cell medium (SFM,
130 contained F-12/DMEM, bFGF, EGF, insulin, and B27), 10-14 days after which primary A549 cell
131 spheres were shaped. Finally we resuspended the primary spheres, and continued to grow in SFM to
132 obtain secondary A549 cell spheres.

133

134 **Synthesis and transfection of PNA-TPP complex**

135 The PNA-TPP sequence designed and synthesized by PNAGENE company (daejeon, korea), was
136 complementary to consensus sequence of human mtDNA L-chain and H-chain in D-loop region, which
137 is 5'-CANACCGCCAAAAGA-3'. Then we transfected PNA-TPP diluted in SFM to a final
138 concentration of 1nmol/mL in A549 cell spheres and incubated at 37°C, 5% CO₂ without light
139 exposure for 24 hours.

140

141 **ATP content determination**

142 ATP content determination was performed following the specification. Briefly, Equal number of
143 cultured cells (>10⁶) was collected for subsequent ATP analyses. The cells were resuspended in hot
144 double-distilled water and cell membranes ruptured in boiling water bath for 10min, then mixed via
145 vortex blending for 1 min to form ATP determination sample. The sample was collected for analyzing
146 ATP by using a ATP Assay Kit (colorimetric). The absorbance was measured at 636 nm with Automatic
147 microplate reader. ATP content was calculated by the following formula: ATP content (μmol/gprot)=
148 (OD value of absorbance of treated group-OD value of absorbance of untreated)/(OD value of
149 absorbance of standard group-OD value of absorbance of blank)*concentration of ATP standard sample
150 (103μmol/L)*sample dilution multiple/sample protein concentration.

151

152 **Western blot analysis**

153 Total cellular proteins of A549 cells and A549 cell spheres under different treatments was isolated
154 using RIPA lysis buffer with phenylmethanesulfony fluoride (PMSF) and mitochondrial proteins were
155 extracted by a mitochondrial protein isolation Kit. The protein concentration was determined by the
156 bicinchoninic acid (BCA) assay. Then proteins were diluted in SDS-PAGE protein loading buffer, a
157 kind of 5× concentrated solution, to working concentration and denatured in boiling water. After that,
158 identical quantity of proteins were electrophoretically separated by 8% or 10% sodiumdodecyl
159 sulfatepolyacrylamide gel electrophoresis (SDS-PAGE) and the protein bands were transferred to
160 polyvinylidene difluoride membrane (PVDF) membranes which blocked in 10% Skim Milk /TBST for
161 1-2 hours at room temperature. The PVDF membranes with protein bands were incubated with
162 appropriate primary antibodies dilute in 5%BSA/TBST at 4 °C overnight. The membranes were
163 incubated with PKA-Cα (1: 500), Drp1 (1: 500), Bcl-2 (1: 1000), Bax (1: 1000) and β-actin (1: 2000).
164 The membranes were washed three times using 1xTBST 10 minutes once a time and incubated with
165 corresponding HRP-conjugated secondary antibodies for 1-2 hours. After washed three times again,
166 protein bands were detected with the ECL detection system and image lab software.

167

168 **Determination of ROS production**

169 Reactive oxygen species generation by astrocytes was detected with the fluorescent probe
170 Dihydroethidium (DHE). Dihydroethidium is a membrane-permeable compound, is oxidized to red
171 fluorescent ethidium (DNA binding membrane-impermeable compound) by the action of radicals (O₂⁻).
172 The A549 cells and A549 cell spheres were incubated with 5 μM of DHE for 30 min at 37°C and
173 protected from light. Finally, intracellular ROS production was determined by the increase in
174 fluorescence observed by an fluorescence microscope under identical conditions in all experimental
175 groups.

176

177 **Design and interfection of lentiviral**

178 Design of DRP1 short hairpin RNA (PL-DNM1L-SH1, PL-DNM1L-SH2, PL-DNM1L-SH3) from
179 invitrogen cloned into lentiviral vector PL/IRES/GFP/U6, (PL-DNM1L-SH1, PL-DNM1L-SH2,
180 PL-DNM1L-SH3) and synthesis of DRP1 (PL-DNM1L) was cloned into lentiviral vector
181 pDS087-pL6-TO-V5-GIM. A549 cell spheres were cultured, subsequently Transfected with lentiviral
182 vector. Cisplatin or PNA-TPP was added 72 hours later. After selection, cells were plated for
183 proliferation and apoptosis.

184

185 **Assessment of proliferation by CCK-8**

186 Cell proliferation was detected with CCK-8 (TransGen Biotech, Beijing, China) according to the
187 manufacturer's instructions. In brief, A549 cell spheres were cultured in 96-well plates with three
188 multiple holes under different treatment, and cell culture absorbance at 450 nm in each well was read
189 by microplate reader after incubation for another 4 h.

190

191 **Annexin V-APC/PI**

192 After different treatments on A549 cell spheres, the percentage of apoptotic cells were determined with
193 the Annexin V-FITC/PI staining following by the manufacturer's instructions. In addition, we used BD
194 flow cytometer to analysis the cells positive after Annexin V-FITC/PI staining for 20min.

195

196 **Statistical analysis**

197 Experimental results of Western Blot were quantitatively analyzed by Image J software. β -actin was
198 used to normalize the values of target protein. Every experiments was redid at least three times.
199 Statistical analysis was performed by SPSS statistics for windows using two tailed Student's t test for
200 comparison of two groups and data were expressed as mean \pm standard deviation (mean \pm SD). In all
201 experiments, if there was a $P < 0.05$, differences were deemed statistically significant.

202

203 **Results**

204

205 **Generation of A549 tumor spheres from A549**

206 A549 cells formed three morphologically different colonies: holoclone, meroclone and paraclone by
207 using single-cell cloning culture. Then, the holoclones were digested only and directly incubation with
208 SFM. Three or four weeks later, A549 cells gradually formed into highly clustered tumor cell spheres,
209 ie, A549 cell spheres (Fig 1). Our experiment shown that A549 cell spheres was higher expression level
210 of PKA-C α and Bcl-2 protein but lower mitochondria Drp1 and Bax than monolayer adherent growth
211 A549 cells (Fig 2).

212

213 **The PNA-TPP reduced the intracellular ATP levels and increased the intracellular ROS level in**
214 **A549 cell spheres**

215 Previous studies in our group showed that the levels of ROS and ATP in A549 cell spheres were lower
216 than those in A549 cells. Most of the intracellular ROS and ATP are dependent on mitochondrial
217 oxidative phosphorylation. Therefore, we designed a peptide nucleic acid-triphenylphosphine
218 complexes (PNA-TPP) targeted to interfere with the A549 cell spheres mitochondrial light and heavy
219 chain consensus sequence 5'-CANACCGCCAAAAGA-3'. After obtaining the corresponding OD value
220 with microplate reader, the intracellular ATP content of A549 cell spheres in the blank control group

221 and PNA-TPP transfection group was calculated to be (125.20 ± 10.90) $\mu\text{mol/gprot}$ and (64.06 ± 7.86)
222 $\mu\text{mol/gprot}$, respectively. That is, PNA-TPP treatment reduced the intracellular ATP levels in A549 cell
223 spheres as shown in Fig. 3. we determined the effect of PNA-TPP on intracellular ROS levels in A549
224 cell spheres using DHE-ROS fluorescence. The IOD values were obtained using Image Pro Plus 6.0
225 software analysis results.

226

227 **PNA-TPP promoted Drp1 recruitment to mitochondrial to enhance cisplatin-induced apoptosis** 228 **in A549 cell spheres via the cAMP/PKA pathway**

229 Many studies have shown that mitochondrial fission is closely related to apoptosis. Studies have shown
230 that disturbing of mitochondrial oxidative phosphorylation can promote apoptosis by affecting
231 cAMP/PKA pathway and mitochondrial fragmentation. Phosphorylation at Drp1 S637 leads to an
232 elongated mitochondrial morphology. Down-regulation of cAMP/PKA pathway can inhibit the
233 phosphorylation of the 637 serine of Drp1, promote the transfer of Drp1 to the mitochondria, and
234 promote mitochondrial fission. To verify this hypothesis, A549 sphere was treated with PNA-TPP for
235 24 hours, and then, the expression of mitochondrial Drp1 was detected. The data showed that the
236 expression of PKA-C α protein in A549 cell spheres was decreased and the expression of mitochondrial
237 Drp1 protein was significantly increased upon PNA-TPP treatment, as compared with control group
238 (Fig. 4 A-D). Additional, we found that PNA-TPP could promote the apoptosis level of A549 cell
239 spheres and enhance the sensitivity to cisplatin. There was no significant change in the expression of
240 bcl-2 and Bax protein between the blank control group and PNA-TPP group. However, compared with
241 PNA-TPP or CDDP treatment alone, the expression level of bcl-2 protein in PNA-TPP combined with
242 cisplatin group was significantly reduced, and the expression level of Bax protein was significantly
243 higher (Fig. 4E-G). CCK8 showed that cell proliferation rate of A549 cell spheres were suppression
244 after PNA-TPP treatment and the PNA-TPP combined with CDDP treatment group was less than that
245 of PNA or CDDP alone treatment group (Fig. 5A, control, 100.0 ± 0 ; PNA-TPP, 76.85 ± 4.72 ; CDDP,
246 74.15 ± 5.99 ; PNA-TPP+CDDP, 51.80 ± 5.13). Cell apoptosis rate of A549 cell spheres by flow
247 cytometry after PNA-TPP treatment was increased and PNA-TPP combined with CDDP treatment
248 group was higher than that of PNA or CDDP alone treatment group (Fig. 5B) control, 6.92 ± 2.74 ;
249 PNA-TPP, 14.44 ± 2.76 ; CDDP, 16.61 ± 2.31 ; PNA-TPP+CDDP, 32.10 ± 5.67).

250

251 **The effect of interfering with expression of Drp1 using lentivirus transfection technology on ROS** 252 **level, the cell proliferation and apoptosis in A549 cell spheres**

253 Drp1 played critical roles in ROS production, cell **apoptosis and** sensitivity to cisplatin. Given the
254 above results, we hypothesized PNA-TPP can elevate levels of ROS, induce cell apoptosis and increase
255 cisplatin chemotherapy sensitivity via regulation of Drp1. To prove this hypothesis, A549 cells were
256 transfected with pLv-Drp1 and sh-Drp1 and selected with blasticidin to establish a stably cell line.
257 Stably transfected cells were cultured in SFM to evaluate the role of Drp1 in A549 cell spheres (Fig.
258 6A-B). Our study showed the expression of Drp1 was increased and suppressed in A549 pLv-Drp1 and
259 sh-Drp1 cell spheres (Fig. 6C-D). Consistent with the effect of PNA-TPP, the ROS level were increased
260 in pLv-Drp1 A549 cell spheres. Similar with PNA-TPP transfection, the cell apoptosis were
261 significantly more accelerated and had a higher proliferative ability in PLv-Drp1 A549 cell spheres
262 than control group, which revealed the opposite result in sh3-Drp1 A549 cell spheres (Fig. 6E-G).

263

264 **Discussion**

265 Currently, cancer stem cells have been widely considered to drive tumorigenesis and tumor growth,
266 drug resistance, and lead to cancer treatment resistance and recurrence. Studies proved that CSCs
267 resistance to Chemotherapy can be obtained by, expression of ATP-binding cassette drug pumps,
268 increased expression of anti-apoptotic proteins, resistance to DNA damaging agents. Our study. our
269 study suggested that A549 cell sphere had the stronger ability of drug resistance, with higher
270 expression of Bcl-2 protein and lower expression level of Bax protein. It was consistent with the above
271 studies²⁰.

272 The results of this study showed that PNA-TPP treatment of lung cancer A549 stem cell spheres,
273 PKA-C α protein expression decreased, mitochondrial Drp1 protein expression increased, the
274 intracellular ATP content decreased. Oxidative phosphorylation of mitochondrial inner membranes
275 produces a majority of intracellular ATP by aerobic metabolism. F1F0-ATP synthase is a key enzyme
276 that regulates ATP production. Two important subunits, ATP6 and ATP8, are transcribed and expressed
277 by mitochondrial DNA¹⁶. Interfering with the mitochondrial DNA promoter consensus reduces the
278 gene expression and inhibits ATP production. Drp1, is the key component of the mitochondrial fission
279 machinery. Drp1 protein is encoded by nuclear DNA, distributed in the cytoplasm and mitochondria.
280 However Drp1 activity is dependent on its activation by different post-translational modifications,
281 including O-GluNACylation, SUMOylation, phosphorylation, S-nitrosylation, and glycosylation, and
282 on the translocation from cytosol to mitochondria²¹. Evidence shows inhibition of the respiratory chain
283 can lead to increased mitochondrial fission^{22,23}. Mitochondrial DNA damage promotes mitochondrial
284 fission, decreased mitochondrial membrane potential, reduced ATP synthesis, and increased release of
285 cytochrome c²³. It has been reported that if silence the death associated protein 3 (DAP3), the synthesis
286 of oxidative phosphorylated protein encoded by mitochondrial DNA and the phosphorylation of Ser
287 637 in Drp1 are reduced, after which the mitochondrial fission promoted, which can reversed by
288 enhancing the activity of PKA²⁴. PKA holoenzyme consists of two regulatory subunits (R subunits) and
289 two catalytic subunits (C subunits), PKA-C α is one of the catalytic subunits. There is no activity in the
290 case of holoenzymes, but it can be hydrolyzed to produce activity under the action of cAMP. A large
291 number of studies have found that PKA-C α is highly expressed in the serum of colorectal, lung,
292 prostate, renal and adrenal glands, and lymphoma patients²⁵. At the same time, it was found that human
293 epidermal growth factor receptor-2 (HER2) is positive, especially for trastuzumab-resistant breast
294 cancer patients with higher PKA-C α protein expression levels²⁶. The above shows that Drp1 and PKA
295 are closely related to energy metabolism and may play a key role in tumorigenesis and drug resistance.
296 Interestingly, activation of the cAMP/PKA signaling pathway activates target genes that play an
297 important role in regulating stem cell self-renewal and differentiation^{27,28}. The experimental results also
298 showed that the level of PKA-C α in A549 cell spheres was higher than that in A549 cells, and the
299 expression of Drp1 protein in mitochondria was reduced. This is consistent with the above findings. At
300 the same time, the SANC study of cardiac sinus node cells found that cAMP synthesis requires the
301 consumption of ATP, and interference with mitochondrial oxidative phosphorylation can reduce cAMP
302 production by inhibiting ATP²⁹. In summary, we believe that the possible mechanism of PNA-TPP
303 inhibiting mitochondrial fission in A549 cell spheres is that PNA-TPP targets mitochondrial oxidative
304 phosphorylation in the mitochondria, reduces ATP production, inhibits cAMP/PKA pathway activation,
305 and mediates Drp1 position 637 Serine phosphorylation is reduced and Drp1 protein is localized in
306 mitochondria, eventually leading to increased mitochondrial fission.

307 The results of this experiment show that when PNA-TPP is targeted to enter the mitochondria,
308 mitochondrial Drp1 protein increases, ROS production also increased, the rate of apoptosis increased,

309 the cell proliferation capacity weakened. Mitochondrial splitting and apoptosis contribute to
310 mitochondrial fission induced by excessive ROS-induced oxidative stress. Lipopolysaccharide (LPS)
311 stimulated the increase of Drp1 protein expression and promoted the mitochondrial fission and ROS
312 production of microglia. The expression of mitochondrial fission inhibitor 1 (Mdivi-1) and silencing
313 Drp1 can reverse the above-mentioned effects of LPS, and then stimulate downstream NF- κ B and
314 MAPK pathways to exert biological effects³⁰. Our study also found that overexpression of Drp1
315 promoted ROS production, decreased cell viability and increased apoptosis, which was similar to
316 PNA-TPP, and down-regulation of Drp1 did the opposite. However, PNA-TPP can also promote ROS
317 production by interfering with mitochondrial energy metabolism. Interfere with chronic lymphoid
318 leukemia cells F1F0-ATPase, promote ROS production and apoptosis³¹. In conclusion, PNA-TPP may
319 partially inhibit mitochondrial fission, promote ROS production, resulting in oxidative stress and
320 promoting apoptosis, nuclear transcription factor kappa B (NF- κ B) and mitogen-activated protein
321 kinase (MAPK) pathway may play a role. However, the specific mechanism needs further study.
322 Currently platinum-based chemotherapy is still the first line of treatment for most lung cancer patients.
323 However, the problem of drug resistance has become increasingly prominent. At present, most studies
324 have confirmed that reversal of drug resistance in tumors depends on mitochondrial fission and
325 increased ROS production. There is a colocalization of Drp1-Bax in the mitochondrial cleavage site,
326 mitochondrial division can decrease Bcl-2 expression and up-regulate Bax, and small interfering RNA
327 (siRNA) inhibits Bax transfer to mitochondria³². However, our results showed that PNA-TPP inhibited
328 mitochondrial fission of lung cancer stem cells, but Bcl-2 protein expression and Bax expression did
329 not change significantly. This may be due to the fact that mitochondrial fission in lung cancer stem
330 cells may affect Bax and Bcl-2 proteins through other proteins other than Drp1, or that Drp1 may
331 promote apoptosis by regulating other apoptosis mechanisms, but its apoptosis mechanism is to be
332 further studied. Studies have shown that by inducing elevated ROS production in rectal cancer cells,
333 down-regulating Bcl-2 and up-regulating Bax protein expression can promote apoptosis, reverse
334 multidrug resistance of rectal cancer, and enhance chemosensitivity³³. This is similar to our
335 experimental results. Our research results indicated compared with PNA-TPP or cisplatin alone, the
336 PNA-TPP combined with cisplatin treatment group expressed higher levels of Bax and lower levels of
337 Bcl-2, and increased apoptosis rate and decreased cell proliferation ability. This suggests that PNA-TPP
338 may enhance cisplatin chemosensitivity by promoting mitochondrial fission and increasing ROS levels.
339 Cisplatin can induce oxidative stress by inducing ROS production during chemotherapy, leading to
340 DNA damage in tumor cells and triggering a cascade of apoptosis-related cascades. Due to cancer stem
341 cells have stronger DNA repair ability, which may be one of the reasons why cisplatin chemotherapy is
342 not sensitive. In this experiment, PNA-TPP was able to induce oxidative stress and cause excessive
343 DNA damage, so that the lung adenocarcinoma A549 stem cell sphere could not be repaired in time.

344

345 **Conclusion**

346 In summary, PNA-TPP may partially regulate the cAMP/PKA/Drp1 pathway, promote mitochondrial
347 division and ROS production, promote apoptosis of lung cancer stem cells, and enhance
348 chemotherapeutic sensitivity of cisplatin. This may provide a theoretical basis for lung adenocarcinoma
349 stem cell targeted therapy.

350

351

352

353 **Ethics approval and consent to participate**

354 This article does not contain any studies with human participants or animals performed by any of the
355 authors.

356

357 **Consent for publication**

358 Informed consent For this type of study, formal consent is not required.

359

360 **Availability of data and materials**

361 The datasets used and/or analyzed during the current study are available from the corresponding author
362 on reasonable request.

363

364 **Competing interests**

365 All authors declare no conflict of interest

366

367 **Funding**

368 This work was supported by the National Natural Science Foundation of China (no 81660493) and
369 Natural Science Foundation of Jiangxi province (no 20202ACBL206019).

370

371 **Authors' contributions**

372 Lixia Xie and Xiaoqun Ye developed and designed the study and analyzed the data and wrote the initial
373 draft of the paper Lixia Xie, Ping Hu, Yong Cheng, Xiaoqun Ye performed the experiments Yong
374 Cheng and Ping Hu performed the statistical analyses All authors accepted the final version of this
375 manuscript for publication

376

377 **Acknowledgements**

378 Not applicable.

379

380 **Author information**

381 *Correspondence: Xiaoqun Ye, Email: 511201663@qq.com. Department of Respiratory Diseases, The
382 Second Affiliated Hospital of Nanchang University, Nanchang, China

383 Lixia Xie, Email: xielixia2030@163.com. Department of Respiratory Diseases, The Second Affiliated
384 Hospital of Nanchang University, Nanchang, China

385

386 **References**

387

388 1 Siegel RL, Miller K D, Jemal A. Cancer statistics, 2019 *CA Cancer J Clin* **2019**, *69*, 7-34

389 2 Phi L T H, Sari I N Yang, Y G Lee, S H Jun, N Kim, K S Lee, Y K Kwon, H Y Cancer Stem Cells
390 (CSCs) in Drug Resistance and their Therapeutic Implications in Cancer. *Treatment Stem Cells Int*
391 **2018**

392 3 Pattabiraman, D R Weinberg, R A Tackling the cancer stem cells - what challenges do they pose? *Nat*
393 *Rev Drug Discov* **2014**, *13*, 497-512

394 4 Lima A R, Santos L, Correia M, Soares P, Sobrinho-Simoes M, Melo M, Maximo V.
395 Dynamin-Related Protein 1 at the Crossroads of Cancer. *Genes (Basel)* **2018**, *9*

396 5 Ye X Q, Li Q, Wang G H, Sun F F, Huang G J, Bian X W, Yu S C, Qian G S. Mitochondrial and
397 energy metabolism-related properties as novel indicators of lung cancer stem cells. *Int J Cancer* **2011**,

398 129, 820-831

399 6 Schrawat A, Samanta S K, Hahm E R, St Croix C, Watkins S, Singh S V. Withaferin A-mediated
400 apoptosis in breast cancer cells is associated with alterations in mitochondrial dynamics.
401 *Mitochondrion* **2019**, *47*, 282-293

402 7 Li S, Wu Y, Ding Y, Yu M, Ai Z. CerS6 regulates cisplatin resistance in oral squamous cell carcinoma
403 by altering mitochondrial fission and autophagy. *J Cell Physiol* **2018**, *233*, 9416-9425

404 8 Boland M L, Chourasia A H, Macleod K F. Mitochondrial dysfunction in cancer. *Front Oncol* **2013**, *3*,
405 292

406 9 Fan Z, Yu H, Cui N, Kong X, Liu X, Chang Y, Wu Y, Sun L, Wang G. ABT737 enhances
407 cholangiocarcinoma sensitivity to cisplatin through regulation of mitochondrial dynamics. *Exp Cell Res*
408 **2015**, *335*, 68-81

409 10 Nielsen P E, Egholm M, Berg R H, Buchardt O. Sequence-selective recognition of DNA by strand
410 displacement with a thymine-substituted polyamide. *Science* **1991**, *254*, 1497-1500

411 11 Hu J, Corey D R. Inhibiting gene expression with peptide nucleic acid (PNA)--peptide conjugates
412 that target chromosomal. DNA *Biochemistry* **2007**, *46*, 7581-7589

413 12 Villa R, Folini M, Lualdi S, Veronese S, Daidone M G, Zaffaroni N. Inhibition of telomerase
414 activity by a cell-penetrating peptide nucleic acid construct in human melanoma cells. *FEBS Lett* **2000**,
415 *473*, 241-248

416 13 Thomas S M, Sahu B, Rapireddy S, Bahal R, Wheeler S E, Procopio E M, Kim J, Joyce S C,
417 Contrucci S, Wang Y, Chiosea S I, Lathrop K L, Watkins S, Grandis J R, Armitage B A, Ly D H.
418 Antitumor effects of EGFR antisense guanidine-based peptide nucleic acids in cancer models. *ACS*
419 *Chem Biol* **2013**, *8*, 345-352

420 14 Yao K, Min J, Zhang G, Yu Z. Study on the inhibitory effect of antisense PNA of telomerase for
421 growth of lung cancer cell lines in vitro. *Zhongguo Fei Ai Za Zhi* **2004**, *7*, 196-198

422 15 Shiraishi T, Eysturskarth J, Nielsen P E. Modulation of mdm2 pre-mRNA splicing by
423 9-aminoacridine-PNA (peptide nucleic acid) conjugates targeting intron-exon junctions. *BMC Cancer*
424 **2010**, *10*, 342

425 16 Spelbrink J N. Functional organization of mammalian mitochondrial DNA in nucleoids: history,
426 recent developments, and future challenges. *IUBMB Life* **2010**, *62*, 19-32

427 17 Filipovska A, Eccles M R, Smith R A, Murphy M P. Delivery of antisense peptide nucleic acids
428 (PNAs) to the cytosol by disulphide conjugation to a lipophilic cation. *FEBS Lett* **2004**, *556*, 180-186

429 18 Muratovska A, Lightowlers R N, Taylor R W, Turnbull D M, Smith R A, Wilce J A, Martin S W,
430 Murphy M P. Targeting peptide nucleic acid (PNA) oligomers to mitochondria within cells by
431 conjugation to lipophilic cations: implications for mitochondrial DNA replication, expression and
432 disease. *Nucleic Acids Res* **2001**, *29*, 1852-1863

433 19 Chen S S, Tu X Y, Xie L X, Xiong L P, Song J, Ye X Q. Peptide nucleic acids targeting
434 mitochondria enhances sensitivity of lung cancer cells to chemotherapy. *Am J Transl Res* **2018**, *10*,
435 2940+

436 20 Naka K, Muraguchi T, Hoshii T, Hirao A. Regulation of reactive oxygen species and genomic
437 stability in hematopoietic stem cells. *Antioxid Redox Signal* **2008**, *10*, 1883-1894

438 21 Loson O C, Song Z, Chen H, Chan D C. Fis1, Mff, MiD49, and MiD51 mediate Drp1 recruitment in
439 mitochondrial fission. *Mol Biol Cell* **2013**, *24*, 659-667

440 22 Otasevic V, Surlan L, Vucetic M, Tulic I, Buzadzic B, Stancic A, Jankovic A, Velickovic K, Golic I,
441 Markelic M, Korac A, Korac B. Expression patterns of mitochondrial OXPHOS components, mitofusin

442 1 and dynamin-related protein 1 are associated with human embryo fragmentation. *Reprod Fertil Dev*
443 **2016**, *28*, 319-327

444 23 Torres-Gonzalez M, Gawlowski T, Kocalis H, Scott B T, Dillmann W H. Mitochondrial
445 8-oxoguanine glycosylase decreases mitochondrial fragmentation and improves mitochondrial function
446 in H9C2 cells under oxidative stress conditions. *Am J Physiol Cell Physiol* **2014**, *306*, C221-229

447 24 Xiao L, Xian H, Lee K Y, Xiao B, Wang H, Yu F, Shen H M, Liou Y C. Death-associated Protein 3
448 Regulates Mitochondrial-encoded Protein Synthesis and Mitochondrial Dynamics. *J Biol Chem* **2015**,
449 *290*, 24961-24974

450 25 Turnham R E, Scott J D. Protein kinase A catalytic subunit isoform PRKACA, History, function and
451 physiology. *Gene* **2016**, *577*, 101-108

452 26 Moody S E, Schinzel A C, Singh S, Izzo F, Strickland M R, Luo L, Thomas S R, Boehm J S, Kim S
453 Y, Wang Z C, Hahn W C. PRKACA mediates resistance to HER2-targeted therapy in breast cancer
454 cells and restores anti-apoptotic signaling. *Oncogene* **2015**, *34*, 2061-2071

455 27 Wang H, Sun T, Hu J, Zhang R, Rao Y, Wang S, Chen R, McLendon R E, Friedman A H, Keir S T,
456 Bigner D D, Li Q J, Wang H, Wang X F. miR-33a promotes glioma-initiating cell self-renewal via PKA
457 and NOTCH pathways. *J Clin Invest* **2014**, *124*, 4489-4502

458 28 Jia B, Madsen L, Petersen R K, Techer N, Kopperud R, Ma T, Doskeland S O, Ailhaud G, Wang J,
459 Amri E Z, Kristiansen K. Activation of protein kinase A and exchange protein directly activated by
460 cAMP promotes adipocyte differentiation of human mesenchymal stem cells. *PLoS One* **2012**, *7*,
461 e34114

462 29 Komai A M, Brannmark C, Musovic S, Olofsson C S. PKA-independent cAMP stimulation of white
463 adipocyte exocytosis and adipokine secretion: modulations by Ca²⁺ and ATP. *J Physiol* **2014**, *592*,
464 5169-5186

465 30 Park J, Choi H, Min J S, Park S J, Kim J H, Park H J, Kim B, Chae J I, Yim M, Lee D S.
466 Mitochondrial dynamics modulate the expression of pro-inflammatory mediators in microglial cells. *J*
467 *Neurochem* **2013**, *127*, 221-232

468 31 Jitschin R, Hofmann A D, Bruns H, Giessl A, Bricks J, Berger J, Saul D, Eckart M J, Mackensen A,
469 Mougiakakos D. Mitochondrial metabolism contributes to oxidative stress and reveals therapeutic
470 targets in chronic lymphocytic leukemia. *Blood* **2014**, *123*, 2663-2672

471 32 Wang P, Wang P, Liu B, Zhao J, Pang QS, Agrawal SG, Jia L, Liu FT. Dynamin-related protein Drp1
472 is required for Bax translocation to mitochondria in response to irradiation-induced apoptosis.
473 *Oncotarget* **2015**, *6*, 22598-22612

474 33 Guo P, Wang SP, Liang W, Wang WJ, Wang HJ, Zhao MM, Liu XW. Salvianolic acid B reverses
475 multidrug resistance in HCT8/VCR human colorectal cancer cells by increasing ROS levels. *Mol Med*
476 *Rep* **2017**, *15*, 724-730

477

478 **Illustration**

479

480 Fig 1 The morphology of A549 cells during different culture phase and (A) A549 cells grew adherently in 10%FBS/DMEM
481 medium. (B) Holoclone derived from single parental cell of A549 cells under 10%FBS/DMEM medium. (C) Primary A549 cell
482 spheres formed in the SFM/F-12 medium. (D) Secondary A549 cell spheres derived from single parental cells of primary A549
483 cell spheres formed in the SFM/F-12 medium. (A, B, C) and D 200× under microscopy.

484

485 Fig 2 The level of Drp1 protein in mitochondria and (PKA-Cα, Bcl-2, Bax) protein were detected on A549 cells and A549 cell
486 spheres. (A) Bands showed the protein expression of Drp1 (upper panel), and COX IV (lower panel). (E) Bands from top to
487 bottom showed the protein expression of PKA-Cα, Bcl-2, Bax and β-actin, respectively. (B) and (C,D,F), The quantification
488 results of the western blot respectively with normalization relative to COX IV or β-actin expression. Data are taken from 3

489 independent experiments and shown as the mean± standard deviation. Comparisons were carried out by Student's t-test. *P<0.05,
490 **P<0.01. A549 cell spheres (sphere) versus A549 cells(A549).

491

492 Fig 3 A and B show the ATP level was reduced and the ROS level was increased in A549 cell spheres with PNA-TPP treatment,
493 respectively. A549 cell spheres were treated with PNA-TPP for 24 hours, then ATP and ROS level was measured in cytosol by
494 ATP and ROS detection kit.

495

496 Fig. 4 The level of Drp1 protein in mitochondria and (PKA- α , Bcl-2, Bax) protein were detected on A549 cell spheres with
497 different treatment. A, The protein expression of Drp1 in mitochondria treatment with or without PNA-TPP in A549
498 cell spheres were detected by Western blot. Representative bands show the protein expression of Drp1 (upper panel) and COX
499 IV (lower panel). B, The protein expression of PKA- α treatment with or without PNA-TPP of A549 cell spheres were detected
500 by Western blot. Representative bands show the protein expression of PKA- α (upper panel) and β -actin (lower panel). E, Bcl-2
501 and Bax levels were determined by Western blotting. A549 spheres were incubated with 0.5 μ g/ml CDDP or PNA-TPP for 24 h.
502 Representative bands show the protein expression of Bcl-2 (first panel), Bax (second panel), and β -actin (lower panel).
503 C, D, F, G, The histograms showing quantification of those bands, normalization relative to COX IV or β -actin expression. The data
504 are presented as the mean± standard deviation. of three separate experiments. (ns) P>0.05, *P<0.05, *P<0.01, ***p<0.001,
505 versus the control group. Mito, mitochondria.

506

507 Fig. 5 A and B show PNA-TPP and CDDP affecting the proliferation and apoptosis of A549 cell spheres. A, CCK-8 showed the
508 cell proliferation inhibition rate while A549 cell spheres were transfected with PNA-TPP for 24 hours, after which 0.5 μ g/ml
509 CDDP for 24 hours. B, A549 cell spheres after different treatments were collected and stained by Annexin-V/PI, percentage of
510 cell apoptosis was determined by flow cytometry. Quantification was performed on three independent experiments. Data are
511 presented as mean ± standard deviation. Data were taken comparisons were carried out by Student's t-test. **P<0.01;
512 ***P<0.01. PNA-TPP, CDDP and PNA-TPP+CDDP versus control, respectively.

513

514 Fig. 6 Overexpression or knockdown of Drp1 in A549 cell spheres affected ROS level, cell proliferation and apoptosis. A and
515 B show the transfection rate was over 80% in all experiments. C and D, Testing the efficiency of pLv-Drp1 and different
516 ShRNAs to knockdown endogenous Drp1 in A549 cell spheres in transiently transfection experiments. E, The ROS level was
517 increased and reduced in A549 cell spheres when overexpression and knockdown Drp1, respectively. F, overexpression and
518 knockdown Drp1 may suppress and promote cell proliferation in A549 cell spheres, respectively. G, overexpression and
519 knockdown Drp1 may promote and suppress apoptosis in A549 cell spheres, respectively. CT, control; D-, Drp1 negative control
520 for overexpression using the pDS087-pL6-TO-V5-GIM vector; D+, Drp1 overexpression using pDS087-pL6-TO-V5-GIM vector;
521 Sh-, negative control for knockdown expression of Drp1 using the PL/IRES/GFP/U6; Sh(1-3)+, Sh-RNAs targeting different
522 regions of Drp1 transcript knockdown expression of Drp1 using the PL/IRES/GFP/U6. Quantification was performed on three
523 independent experiments. Data are presented as mean ± standard deviation. Data were taken comparisons were carried out by
524 Student's t-test. (ns) P>0.05, *P<0.05, *P<0.01, ***p<0.001 **P<0.01; D- and Sh- versus CT, respectively, D+ versus D-, Sh-
525 versus Sh(1-3)+.

526

Figures

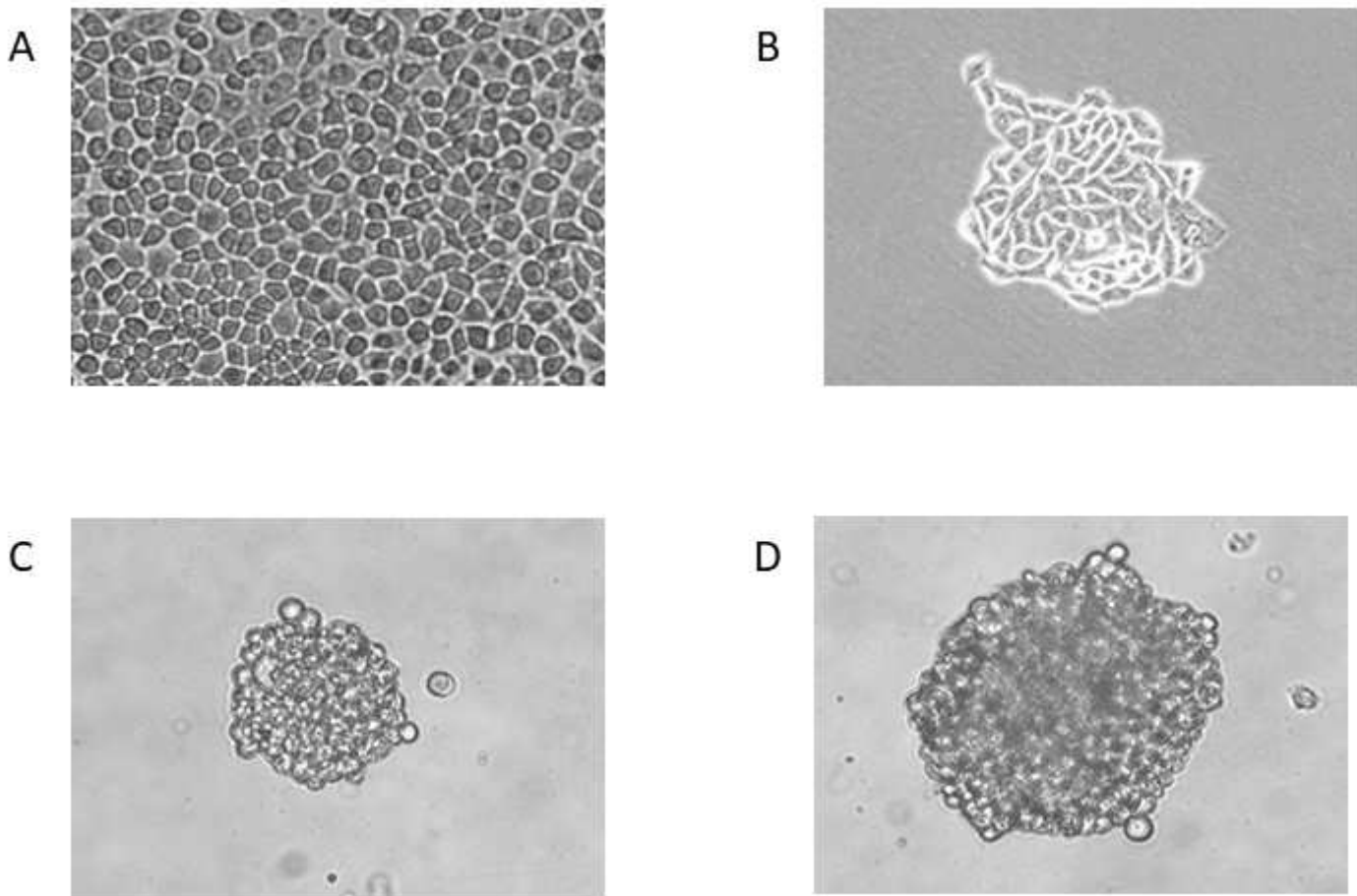


Figure 1

The morphology of A549 cells during different culture phase and (A) A549 cells grew adherently in 10%FBS/DMEM medium. (B) Holoclone derived from single parental cell of A549 cells under 10%FBS/DMEM medium. (C) Primary A549 cell spheres formed in the SFM/F-12 medium. (D) Secondary A549 cell spheres derived from single parental cells of primary A549 cell spheres formed in the SFM/F-12 medium. (A, B, C) and D 200× under microscopy.

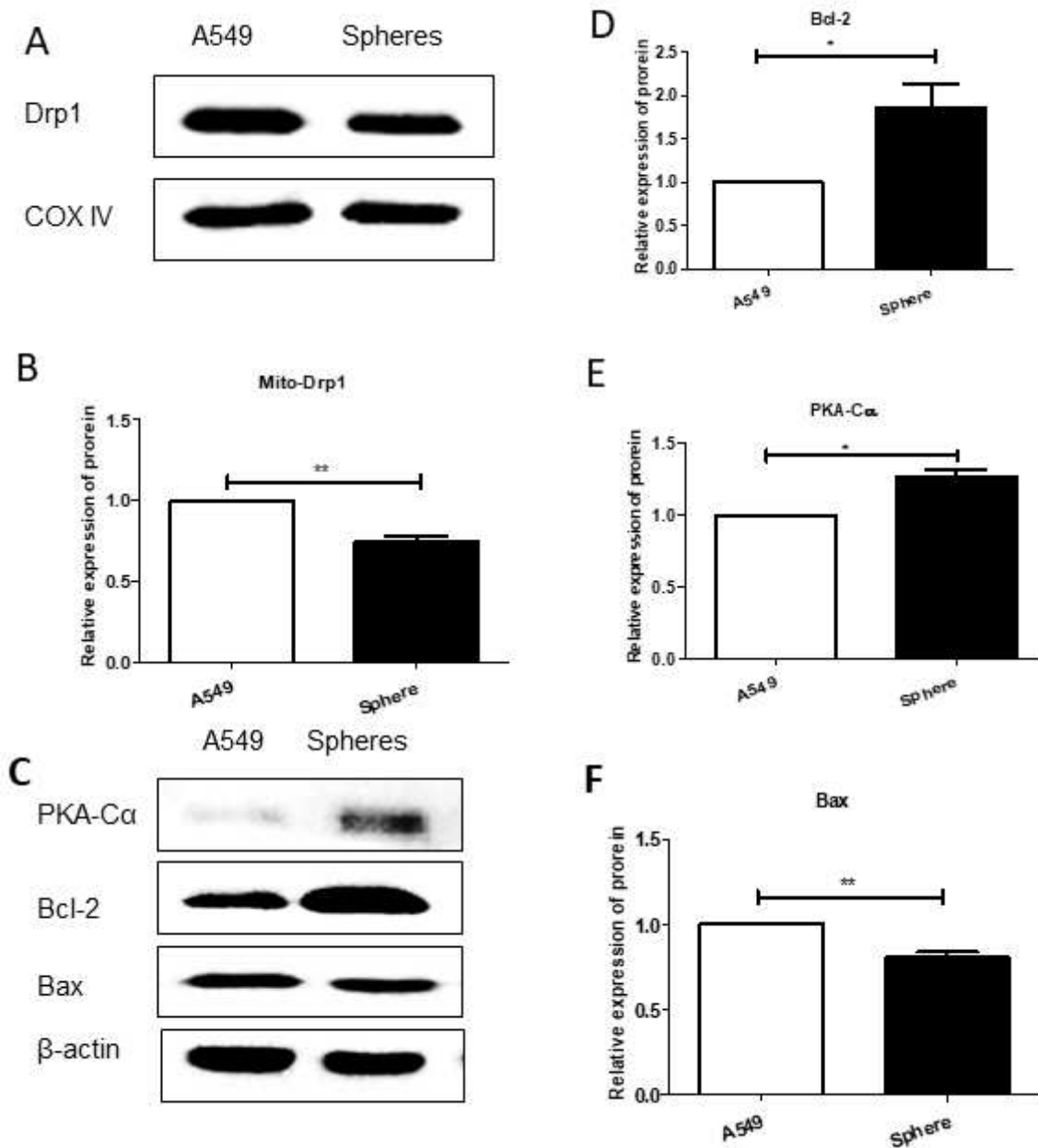


Figure 2

The level of Drp1 protein in mitochondria and (PKA-Cα, Bcl-2, Bax) protein were detected on A549 cells and A549 cell spheres. (A) Bands showed the protein expression of Drp1 (upper panel), and COX IV (lower panel). (E) Bands from top to bottom showed the protein expression of PKA-Cα, Bcl-2, Bax and β-actin, respectively. (B) and (C,D,F), The quantification results of the western blot respectively with normalization relative to COX IV or β-actin expression. Data are taken from 3 independent experiments and shown as the mean ± standard deviation. Comparisons were carried out by Student's t-test. *P<0.05, 489 **P<0.01. A549 cell spheres (sphere) versus A549 cells(A549).

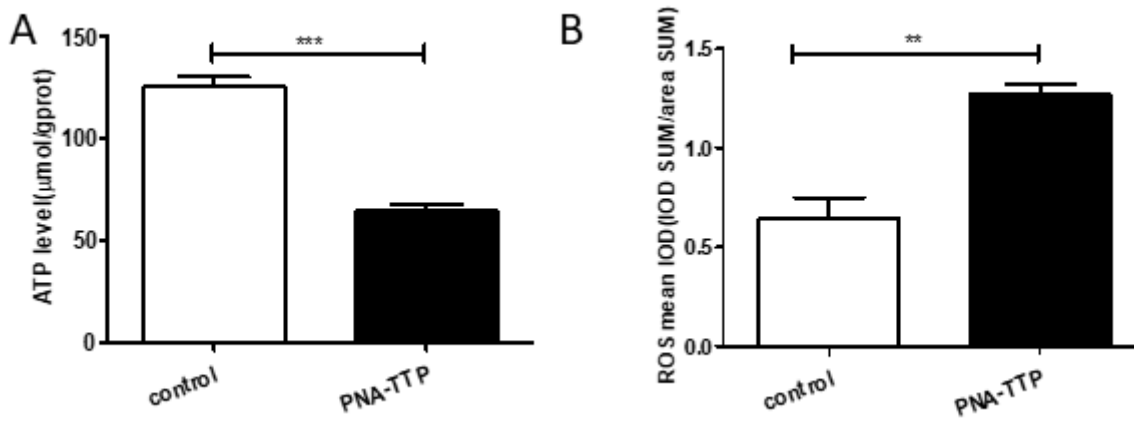


Figure 3

A and B show the ATP level was reduced and the ROS level was increased in A549 cell spheres with PNA-TTP treatment, respectively. A549 cell spheres were treatment with PNA-TTP for 24 hours, then ATP and ROS level was measured in cytosol by ATP and ROS detection kit.

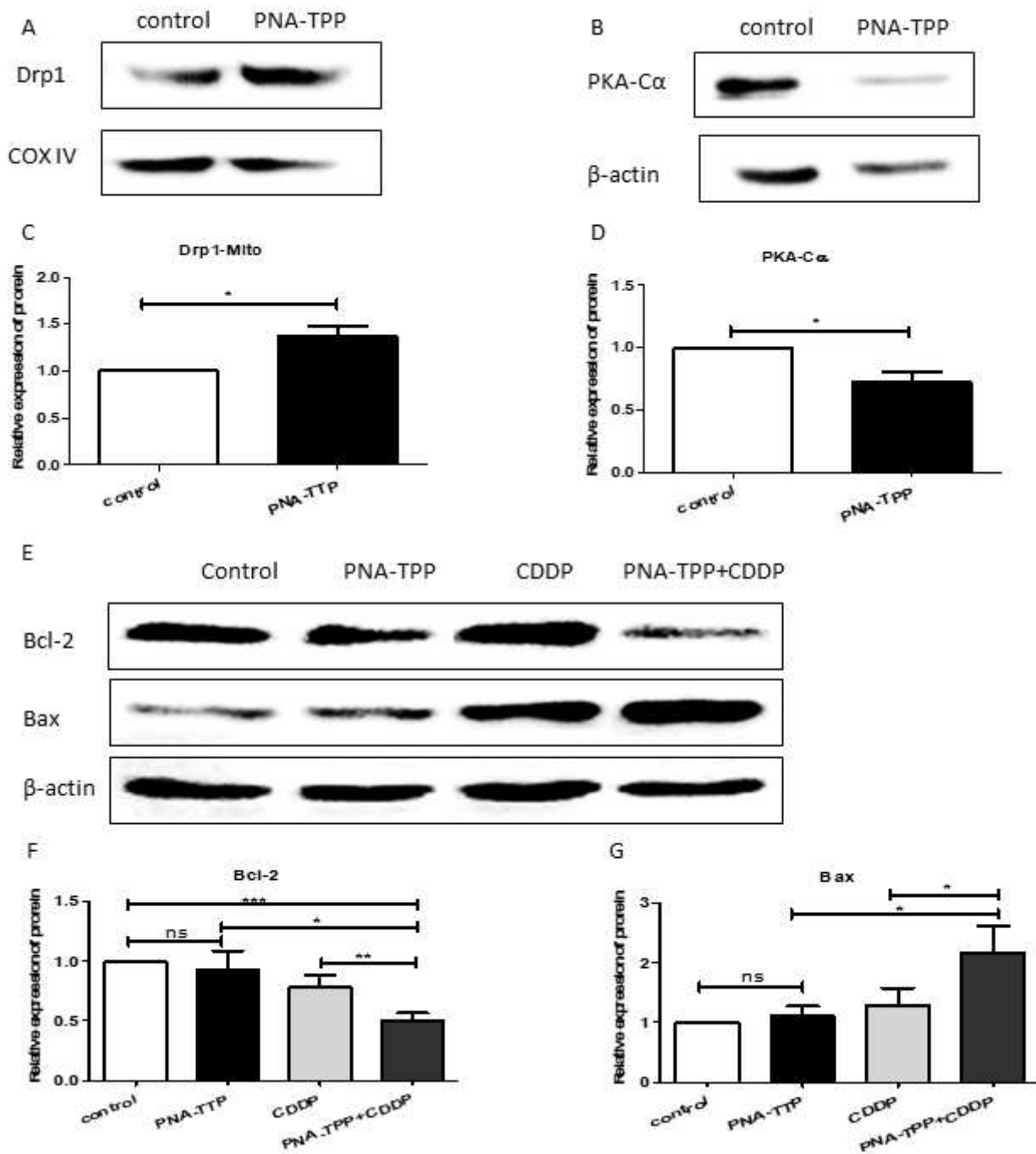


Figure 4

The level of Drp1 protein in mitochondria and (PKA-Cα, Bcl-2, Bax) protein were detected on A549 cell spheres with different treatment. A, The protein expression of Drp1 in mitochondria treatment with or without PNA-TPP in A549 cell spheres were detected by Western blot. Representative bands show the protein expression of Drp1 (upper panel) and COX IV (lower panel). B, The protein expression of PKA-Cα treatment with or without PNA-TPP of A549 cell spheres were detected by Western blot. Representative bands show the protein expression of PKA-Cα (upper panel) and β-actin (lower panel). E, Bcl-2 and Bax levels were determined by Western blotting. A549 spheres were incubated with 0.5 μg/ml CDDP or PNA-TPP for 24 h. Representative bands show the protein expression of Bcl-2 (first panel), Bax (second panel),

and β -actin (lower panel). C,D,F,G,The histograms showing quantification of those bands, normalization relative to COX IV or β -actin expression. The data are resented as the mean \pm standard deviation. of three separate experiments. (ns) $P > 0.05$, * $P < 0.05$, ** $P < 0.01$, *** $p < 0.001$, versus the control group.Mito, mitochondria.

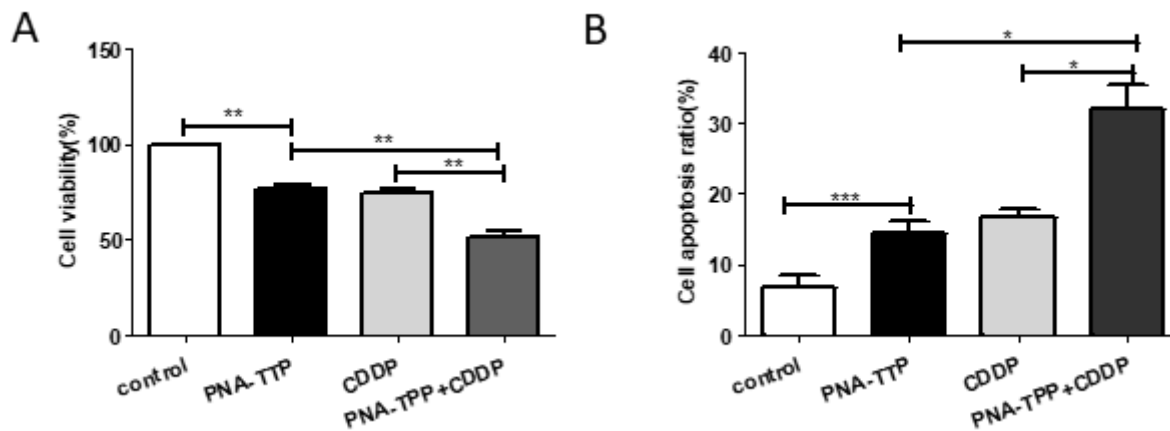


Figure 5

A and B show PNA-TTP and CDDP affecting the proliferation and apoptosis of A549 cell spheres. A, CCK-8 showed the cell proliferation inhibition rate while A549 cell spheres were transfected with PNA-TTP for 24 hours, after which 0.5 μ g/ml CDDP for 24 hours. B, A549 cell spheres after different treatments were collected and stained by Annexin-V/PI, percentage of cell apoptosis was determined by flow cytometry. Quantification was performed on three independent experiments. Data are presented as mean \pm standard deviation. Data were taken comparisons were carried out by Student's t-test. ** $P < 0.01$; *** $P < 0.001$. PNA-TTP, CDDP and PNA-TTP+CDDP versus control, respectively.

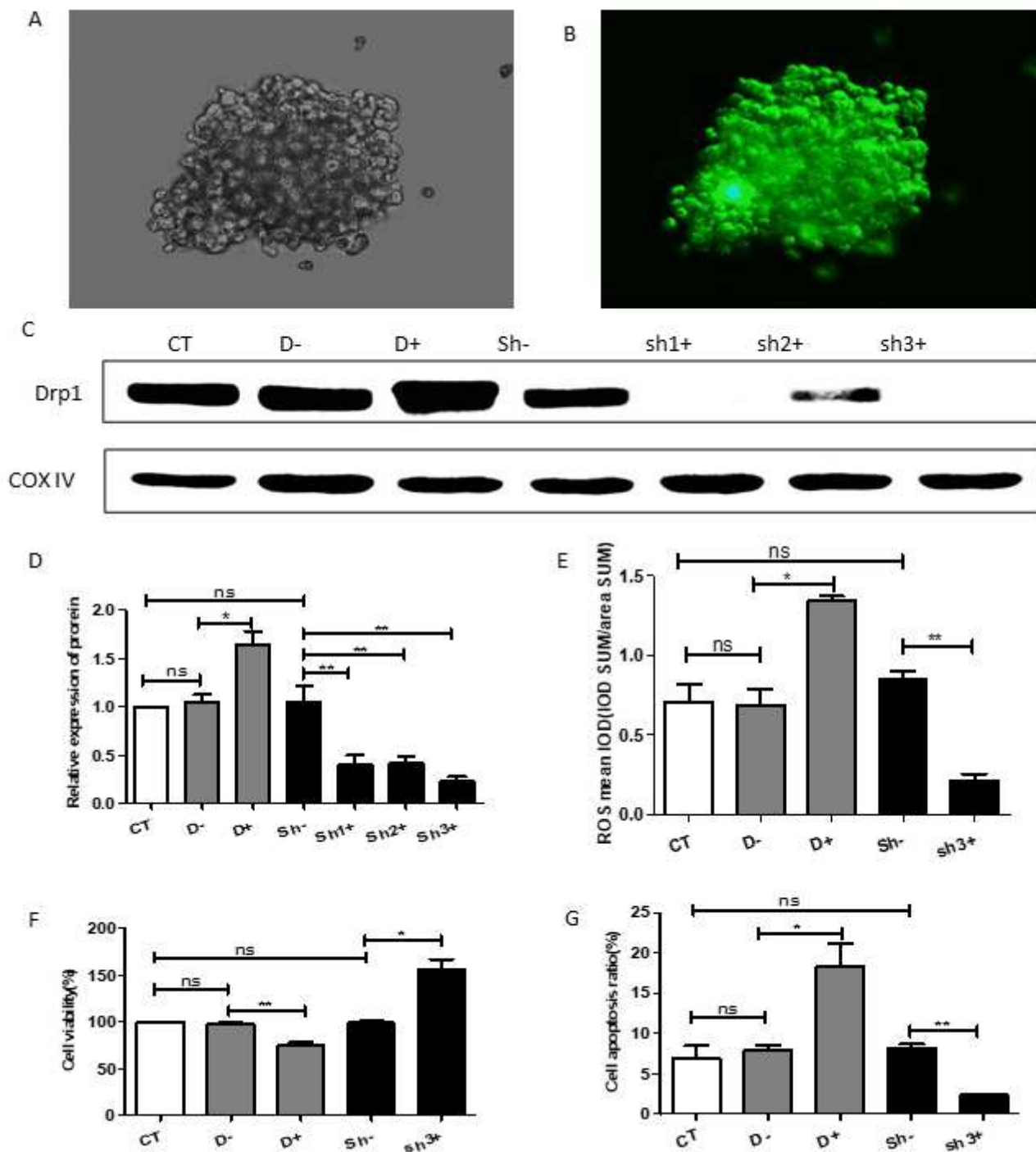


Figure 6

Overexpression or knockdown of Drp1 in A549 cell spheres affected ROS level, cell the proliferation and apoptosis. A and B show the transfection rate was over 80% in all experiments. C and D, Testing the efficiency of pLv Drp1 and different ShRNAs to knockdown endogenous Drp1 in A549 cell spheres in transiently transfection experiments. E, The ROS level was increased and reduced in A549 cell spheres when overexpression and knockdown Drp1, respectively. F, overexpression and knockdown Drp1 may suppress and promote cell proliferation in A549 cell spheres, respectively. G, overexpression and knockdown Drp1 may promote and suppress apoptosis in A549 cell spheres, respectively. CT, control; D-,

Drp1 negative control for overexpression using the pDS087 pL6 TO V5 GIM vector; D+, Drp1 overexpression using pDS087 pL6 TO V5 GIM vector; Sh-, negative control for knockdown expression of Drp1 using the PL/IRES/GFP/U6; Sh(1-3)+, Sh RNAs targeting different regions of Drp1 transcript knockdown expression of Drp1 using the PL/IRES/GFP/U6. Quantification was performed on three independent experiments. Data are presented as mean \pm standard deviation. Data were taken comparisons were carried out by Student's t-test. (ns) P 0.05,*P<0.05,*P<0.01,***p<0.001 **P<0.01;D- and Sh- versus CT ,respectively,D+ versusD-,Sh- versus Sh(1-3)+.